Supplemental Document for

Ion Density-enhanced Electrostatic Precipitation using High Voltage Nanosecond Pulses

Boxin Zhang[4], Indu Aravind[1], Sisi Yang[1], Sizhe Weng[3], Bofan Zhao[3], Grace Johnson[5,6], Lucas Brown[5,6], Jason Olfert[7], Heejung Jung[5,6], and Stephen B. Cronin[1, 2, 3]

[1]Department of Physics and Astronomy, [2]Department of Chemistry, [3]Ming Hsieh Department of Electrical Engineering, [4]Mork Family Department of Chemical Engineering and Materials Science, University of Southern California, Los Angeles, CA 90089, USA

[5]Department of Mechanical Engineering, [6]College of Engineering-Center for Environmental Research and Technology (CE-CERT), University of California, Riverside, Riverside, CA 92521, USA, [7]Department of Mechanical Engineering, University of Alberta, Edmonton, Alberta, Canada

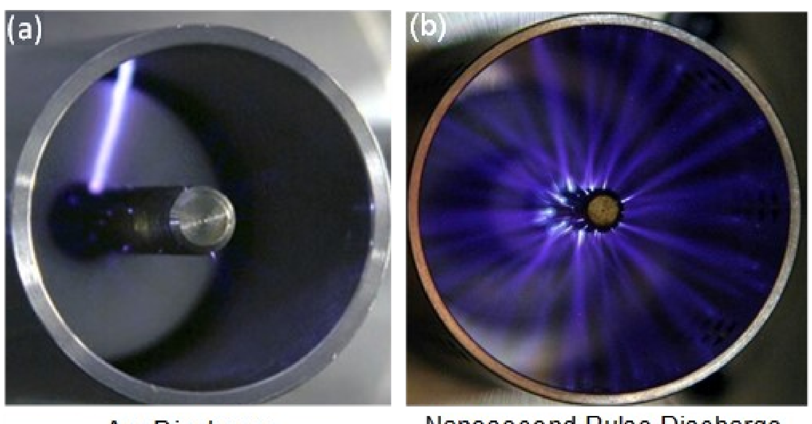

Figure S1. Photograph illustrating the *arcing threshold* in a cylindrical electrostatic precipitator.

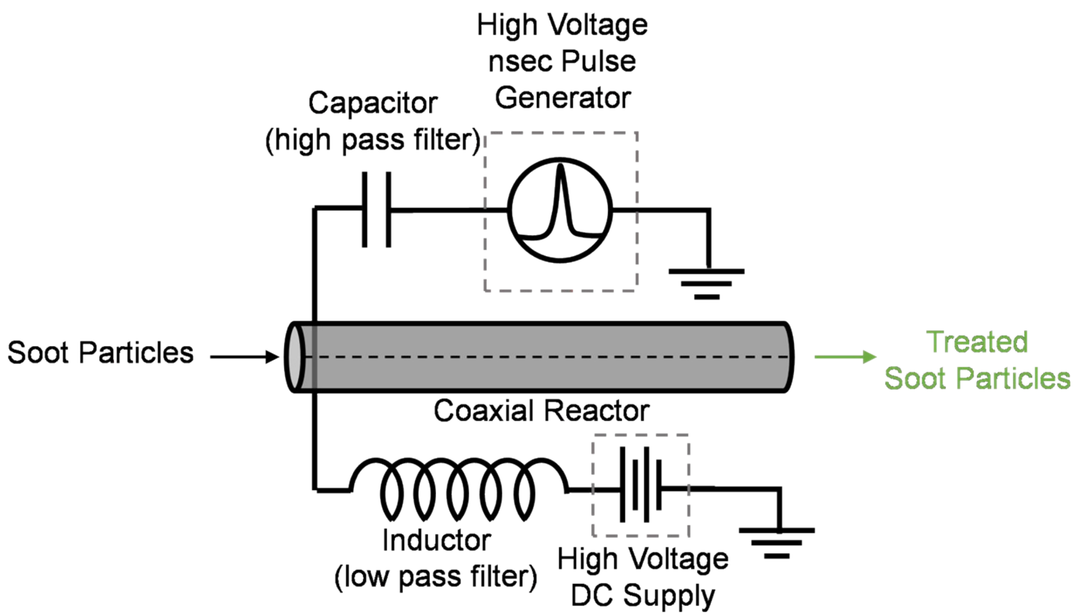

Figure S2. Schematic circuit diagram for nanosecond high voltage pulse generator and high voltage DC power supply.

S1. Measurement of soot effective density

The relationship between particle size and particle mass can be expressed as:

$$m = k d_m^{D_m} \qquad \text{S1}$$

where m is the mass of a particle, k is the mass-mobility pre-factor, d_m is the particle mobility diameter, and D_m is the mass-mobility exponent. The relationship can also be expressed as the 'effective density', ρ_{eff}, defined as

$$\rho_{eff} \equiv \frac{m}{\pi d_m^3/6} = \left(\frac{6k}{\pi}\right) d_m^{D_m - 3}. \qquad \text{S2}$$

The effective density of the soot particles was measured using a DMA (TSI Model 3080), which classifies particles by electrical mobility, in series with a centrifugal particle mass analyzer (CPMA, Cambustion Ltd), which classifies particles by mass-to-charge ratio, and a CPC (TSI Model 3750), as shown in Figure 1 of the manuscript.

In this system, the DMA is set to select a single mobility and the CPMA is stepped through a range of masses while a CPC is used to measure the concentration of particles exiting the CPMA. The resulting particle number-mass distribution is fit with a lognormal distribution to determine the median particle mass for the given DMA mobility diameter. Repeating this procedure over a range of DMA set points gives the relationship between the mass and mobility of the particles (or the effective density as a function of mobility diameter).

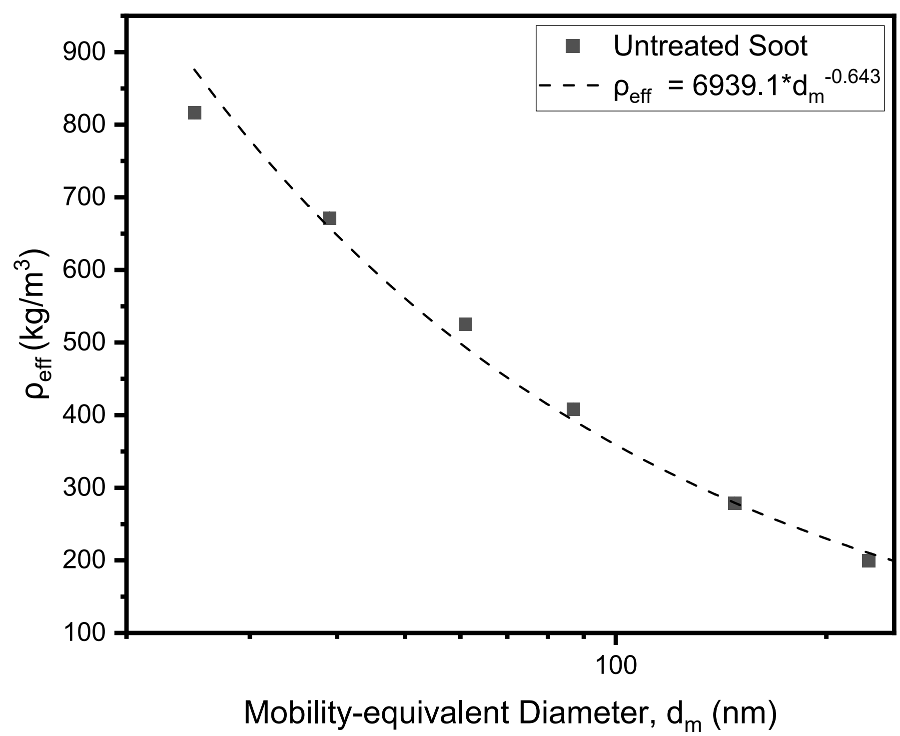

Figure S3. Particle effective density of the untreaded soot.

Figure S3 shows particle effective density of the baseline soot. The results show an effective density profile for the ethylene diffusion flame soot. The effective densities and mass-mobility exponents (2.36) of the soot measured here are typical of soot from other combustion sources (see Olfert and Rogak (2019)[1] for a review of soot effective densities from automotive engines, gas turbines and a wide range of premixed and non-premixed burners).

The particle number-size distributions measured by the SMPS can then be converted to particle mass-size distributions using the effective density relationship. The mass-size distributions are then integrated to calculate the total mass concentration so that the remediation efficiency on a mass basis is found.

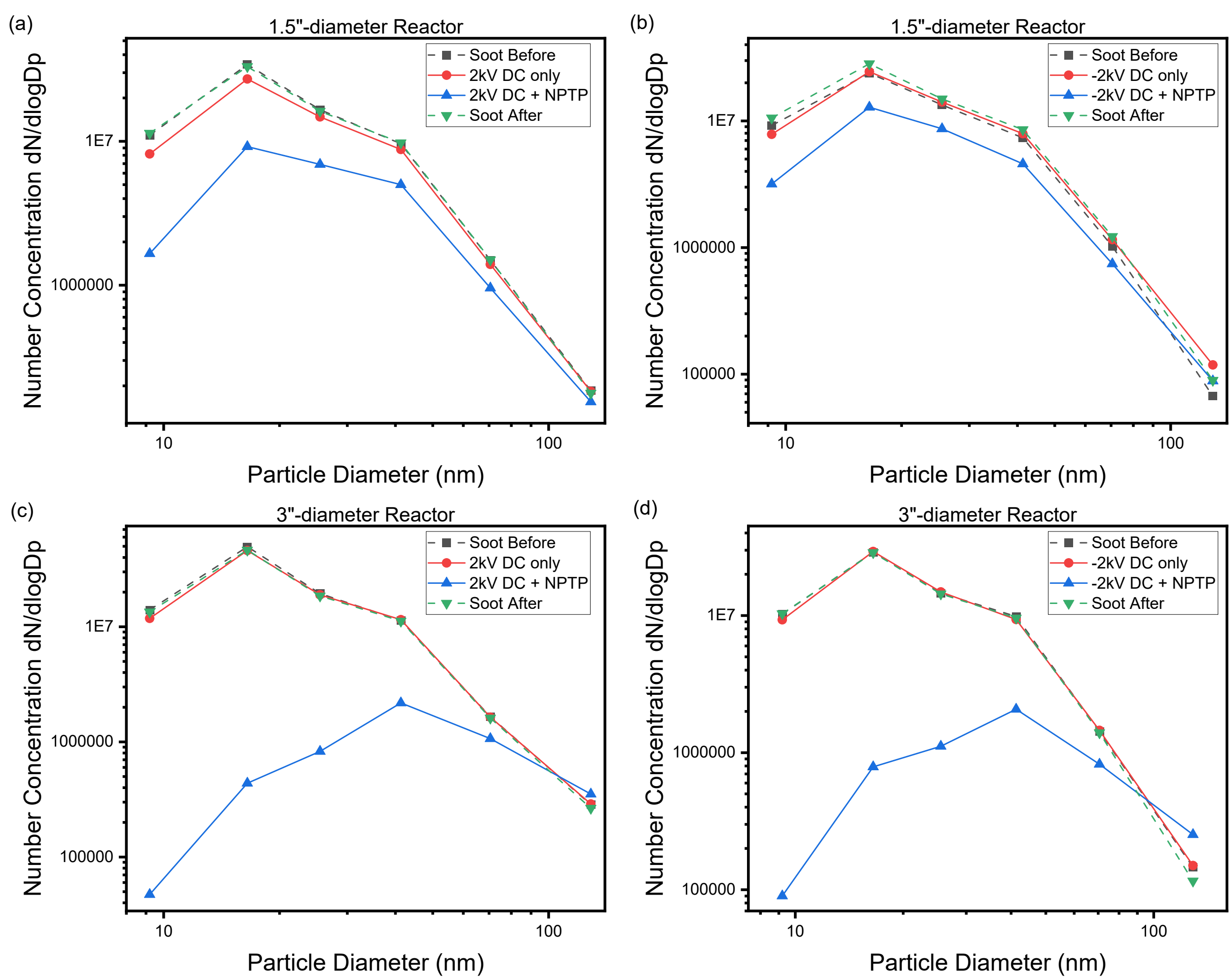

Figure S4. Number concentration vs. Particle diameter plots with (a, b) a 1.5”-diameter reactor, and (c, d) a 3”-diameter reactor. (a) and (c) correspond to positive DC voltage and (b) and (d) correspond to negative DC voltage.

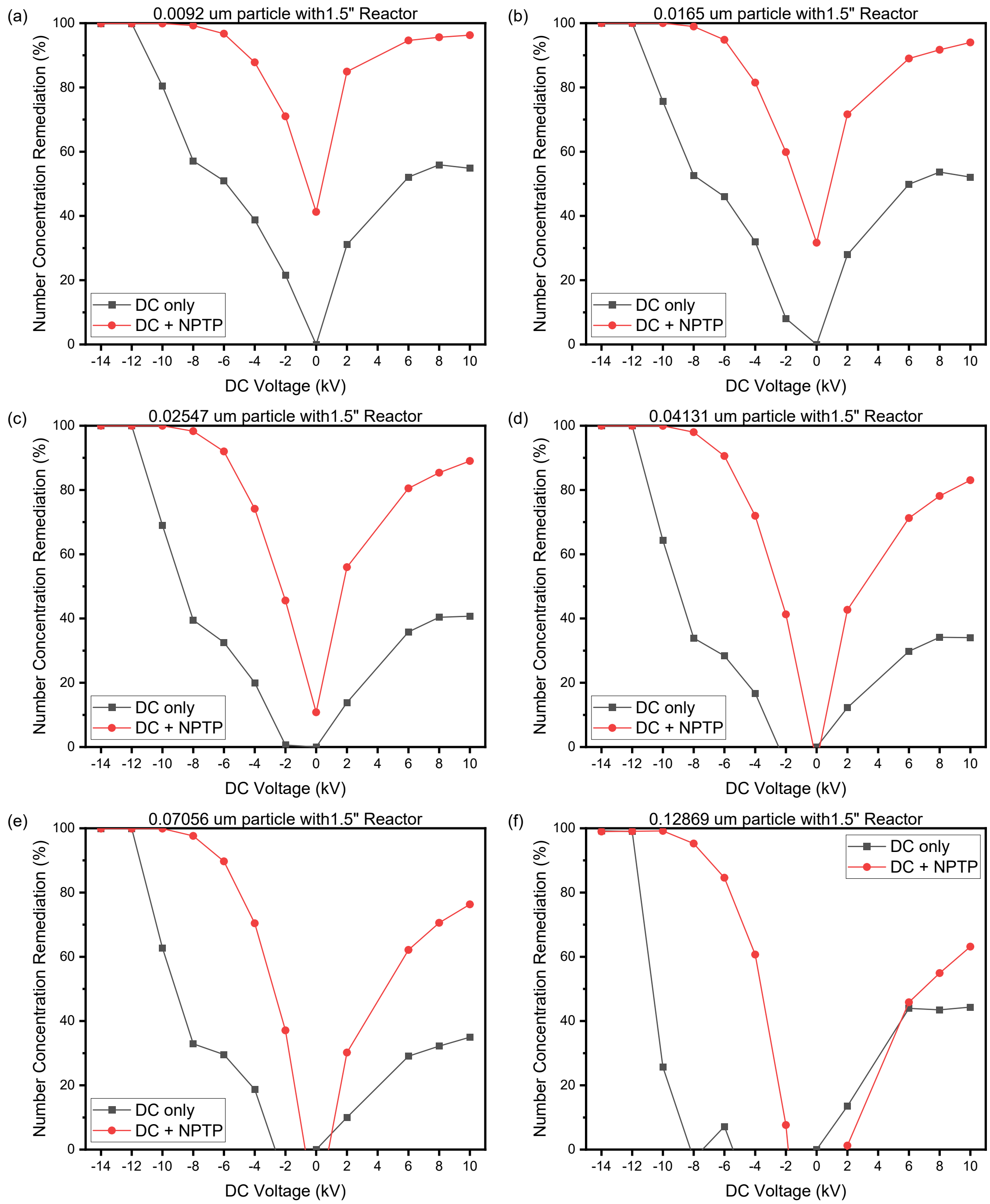

Figure S5. Number concentration remediation percentage for each diameter of nanoparticles with the 1.5”-diameter reactor.

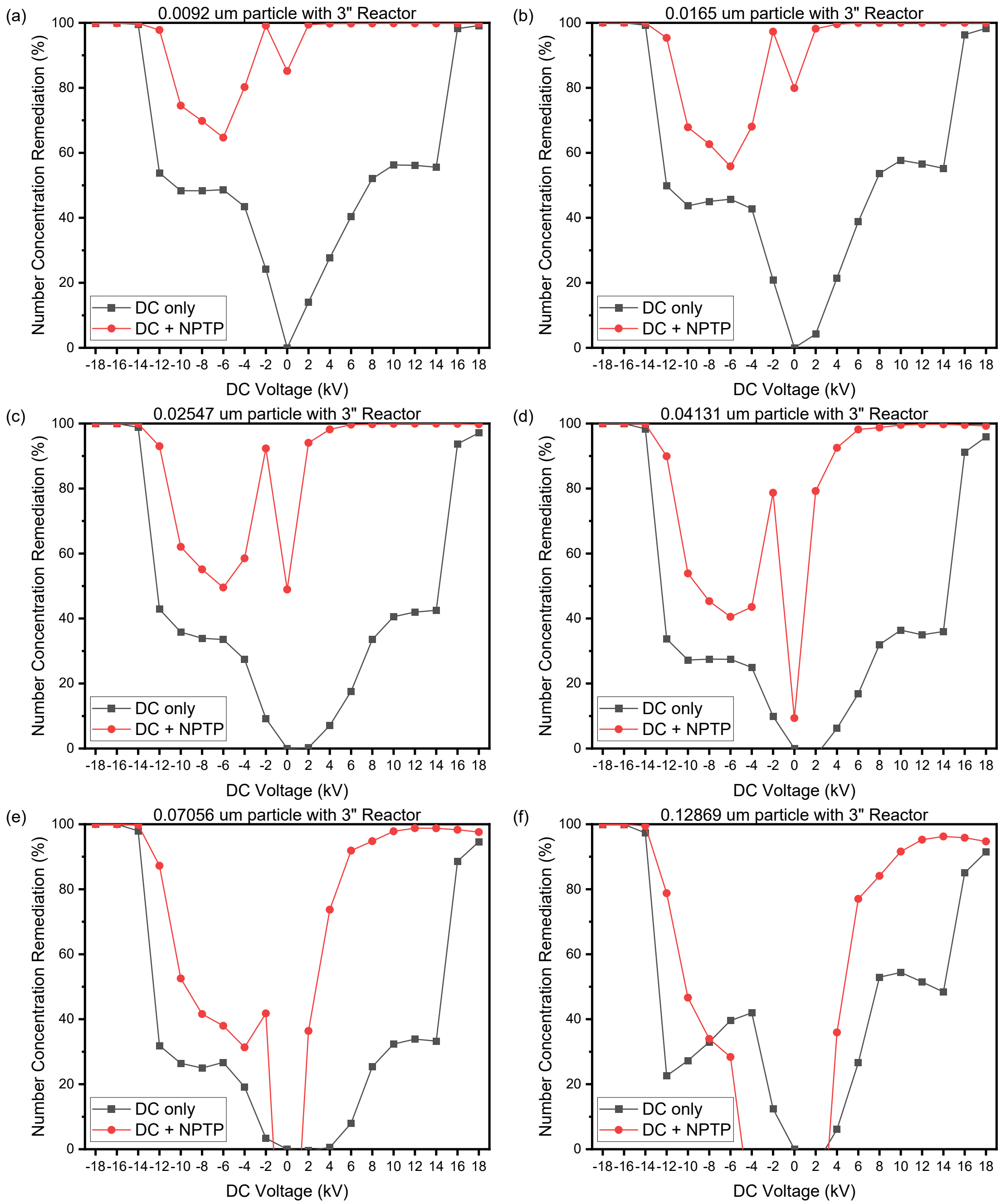

Figure S6. Number concentration remediation percentage for each diameter of nanoparticles with the 3”-diameter reactor.

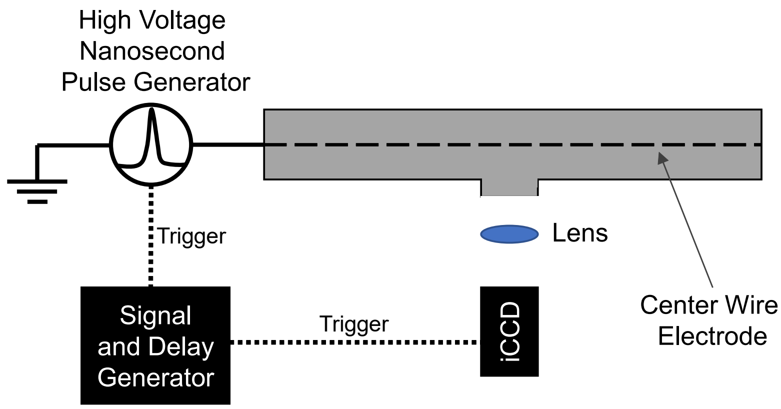

Figure S7. Illustration of iCCD camera and nsec pulse generator configuration for high speed integrated imaging.

References

1. Olfert, J. and S. Rogak, *Universal relations between soot effective density and primary particle size for common combustion sources.* Aerosol Science and Technology, 2019. **53**(5): p. 485-492.